Title

Crosstalk among IL-23 and DNAX Activating Protein of 12 kDa-Dependent Pathways Promotes Osteoclastogenesis

Journal

The Journal of Immunology, 194(1)

ISSN

0022-1767 1550-6606

Authors

Shin, H.-S.
Sarin, R.
Dixit, N.
et al.

Publication Date

2014-12-01

DOI

10.4049/jimmunol.1401013

Peer reviewed

Current Issue: January 1, 2015

The Journal of Immunology

Crosstalk among IL-23 and DNAX Activating Protein of 12 kDa –Dependent Pathways Promotes Osteoclastogenesis

Hyun-Seock Shin, Ritu Sarin, Neha Dixit, Jian Wu, Eric Gershwin, Edward P. Bowman and Iannis E. Adamopoulos

J Immunol 2015; 194:316-324; Prepublished online 1 December 2014;
doi: 10.4049/jimmunol.1401013
http://www.jimmunol.org/content/194/1/316

The Journal of Immunology is published twice each month by
The American Association of Immunologists, Inc.,
9650 Rockville Pike, Bethesda, MD 20814-3994.

Print ISSN: 0022-1767 Online ISSN: 1550-6606.

Crosstalk among IL-23 and DNAX Activating Protein of 12 kDa–Dependent Pathways Promotes Osteoclastogenesis

Hyun-Seock Shin,* Ritu Sarin,* Neha Dixit,* Jian Wu,† Eric Gershwin,* Edward P. Bowman,‡ and Iannis E. Adamopoulos*,§

IL-23 has been well studied in the context of T cell differentiation; however, its role in the differentiation of myeloid progenitors is less clear. In this paper, we describe a novel role of IL-23 in myeloid cell differentiation. Specifically, we have identified that in human PBMCs, IL-23 induces the expression of MDL-1, a PU.1 transcriptional target during myeloid differentiation, which orchestrates osteoclast differentiation through activation of DNAX activating protein of 12 kDa and its ITAMs. The molecular events that lead to the differentiation of human macrophages to terminally differentiated osteoclasts are dependent on spleen tyrosine kinase and phospholipase Cγ2 phosphorylation for the induction of intracellular calcium flux and the subsequent activation of master regulator osteoclast transcription factor NFATc1. IL-23–elicited osteoclastogenesis is independent of the receptor activator of NF-κB ligand pathway and uses a unique myeloid DNAX activating protein of 12 kDa–associated lectin-1$^+$/DNAX activating protein of 12 kDa$^+$ cell subset. Our data define a novel pathway that is used by IL-23 in myeloid cells and identify a major mechanism for the stimulation of osteoclastogenesis in inflammatory arthritis. ***The Journal of Immunology*****, 2015, 194: 316–324.**

The mononuclear phagocyte system consists of a population of cells derived from progenitor cells in the bone marrow, which differentiate to form neutrophils and monocytes and contribute to immunosuppression, disease resolution, and tissue repair (1). M-CSF signaling through its receptor promotes the differentiation of myeloid progenitors into heterogeneous populations of monocytes, macrophages, dendritic cells, and bone-resorbing osteoclasts (2). On the contrary to disease resolution, myeloid populations elicited by M-CSF are also associated with exacerbation of a broad spectrum of pathologies, including cancer, inflammation, and bone disease (3).

M-CSF and receptor activator of NF-κB ligand (RANKL) are essential for the differentiation of osteoclasts from human bone marrow and circulating monocyte precursors (4–6). Proinflammatory mediators such as IL-17 have also been observed to contribute to the proliferation and differentiation of myeloid progenitors (7–9). IL-17 is mainly secreted by Th17 cells, and the differentiation of these Th17 cells is largely regulated by IL-23 (10). We have previously shown that gene transfer of IL-23 in rodents induces myelopoiesis, which also results in severe bone destruction (11). IL-23 is predominantly expressed by monocytes and dendritic cells and acts via IL-23R, which is expressed at low levels on monocytes (12–14). As IL-23R is also expressed on CD4$^+$ T cells, the actions of IL-23 in osteoclast differentiation from myeloid precursors have been largely overshadowed by the ability of Th17 cells to produce RANKL, and hence the interactions of IL-23 with IL-23R$^+$ myeloid cells are only partly known (15). In this paper, we sought to examine the cellular and molecular mechanisms that regulate IL-23–induced osteoclast differentiation in myeloid cells.

T cells and myeloid cells share a requirement for costimulatory signals that are mediated by ITAMs. The ITAM is a conserved signaling motif contained in the cytoplasmic domain of transmembrane adaptor molecules that associate with and transmit signals from various immunoreceptors. In myeloid cells, immunoreceptors signal through two main ITAM-containing adaptors, the DNAX activating protein of 12 kDa (DAP12) and FcRγ, to regulate osteoclastogenesis. Double deletion of DAP12 and FcRγ in mice leads to impaired osteoclast differentiation and osteopetrosis (16). Deletions in the DAP12 gene in humans causes Nasu-Hakola disease, which is characterized by bone fractures and presenile dementia (17). DAP12 associates with multiple immunoreceptors in myeloid precursors including myeloid DAP12-associated lectin (MDL)-1. MDL-1 is a type II transmembrane protein that belongs to the C-type lectin superfamily. It is exclusively expressed in monocytes, macrophages, and dendritic cells and contains a charged residue in the transmembrane region that enables it to pair with DAP12 (18). The ligation of ITAM-coupled receptors in myeloid cells leads to the phosphorylation of ITAM tyrosine residues by SRC family kinases, followed by the recruitment and activation of the spleen tyrosine kinase (SYK) (19). ITAM-coupled receptors and cytokine receptors were shown to be linked by calcium-mediated signaling pathways, and the ITAM-dependent activity of calcium-dependent calmodulin kinase and protein tyrosine kinase 2 were found to augment IFN-induced JAK (and STAT1) activation (20).

*Department of Internal Medicine, Division of Rheumatology, Allergy and Clinical Immunology, University of California, Davis, Davis, CA 95616; †Division of Gastroenterology and Hepatology, Department of Internal Medicine, University of California Davis Medical Center, Sacramento, CA 95817; ‡Discovery Research, Department of Immunology and Immunomodulatory Receptors, Merck Research Laboratories, Palo Alto, CA 94304; and §Institute for Pediatric Regenerative Medicine, Shriners Hospitals for Children–Northern California, Sacramento, CA 95817

Received for publication April 23, 2014. Accepted for publication October 25, 2014.

This work was supported by National Institutes of Health Research Grant R01 AR062173 (to I.E.A.).

Address correspondence and reprint requests to Dr. Iannis E. Adamopoulos, Institute for Pediatric Regenerative Medicine, Shriners Hospitals for Children–Northern California, 2425 Stockton Boulevard, Room 653A, Sacramento, CA 95817. E-mail address: iannis@ucdavis.edu

The online version of this article contains supplemental material.

Abbreviations used in this article: DAP12, DNAX activating protein of 12 kDa; MDL, myeloid DNAX activating protein of 12 kDa–associated lectin; MMP9, matrix metallopeptidase 9; NFATc1, NFAT cytoplasmic 1; OPG, osteoprotegerin; PLCγ2, phospholipase Cγ2; RANKL, receptor activator of NF-κB ligand; sRANKL, soluble RANKL; SYK, spleen tyrosine kinase; TRAP, tartrate-resistant acid phosphatase.

www.jimmunol.org/cgi/doi/10.4049/jimmunol.1401013

In this manuscript, we describe a novel interaction of IL-23 signaling with ITAM-coupled receptors in human $CD16^+$/MDL-1^+/$DAP12^+$ cell subsets. These interactions lead to the phosphorylation of SRC, recruitment of SYK, and activation of NFAT cytoplasmic 1 (NFATc1) to induce the terminal differentiation of these progenitor cells to osteoclasts (16, 21–26). Our data define a novel pathway that is used by IL-23 in myeloid cells and identify a major mechanism for the stimulation of osteoclastogenesis in inflammatory arthritis.

Materials and Methods

Reagents and Abs

Soluble RANKL (sRANKL), osteoprotegerin (OPG), IL-23, TNF, RANKL ELISA, and anti–MDL-1/CLEC5A Ab (283834) were purchased from R&D Systems. Anti–phospho-SYK (Y525/526, Y323, Y352), anti–phospholipase Cγ2 (PLCγ2; polyclonal), and anti–phospho-PLCγ2 (Y759) Abs were purchased from Cell Signaling Technology. Anti-SYK Ab (SYK-01) was purchased from Abcam. Anti-GAPDH, (6C5) anti-SRC (GD11), anti–phospho-SRC (Y418), and anti-phosphotyrosine (4G10) Abs were purchased from Millipore. Anti-human CD16 PE-Cy7 (clone CB16), isotype mouse IgG1κ, and anti-human CD16 PE-Cy5 (clone 3G8) and isotype mouse IgG1 PE-Cy5 were from eBioscience and BioLegend, respectively. Anti-human CD14 FITC and isotype mouse IgG1 FITC were from BioLegend. Anti-human DAP12-PE and isotype control rat IgG1 PE were purchased from Beckman Coulter and eBioscience, respectively. Anti-NFATc1 Ab (7A6) was purchased from Thermo Scientific. Anti-DAP12 Ab (406288) was purchased from Exalpaha. Anti–IL-23R (H-300) was purchased from Santa Cruz Biotechnology.

Surface and intracellular staining

For surface staining, 5×10^6 PBMCs was blocked with 2% FBS in PBS and then stained with CD14-FITC, CD16 PE-Cy7, or MDL-1–allophycocyanin with appropriate isotype controls on ice for 30 min. Cells were then washed with FACS buffer. Cells were acquired on a DAKO Cyan (DakoCytomation) or FACSAria (BD Biosciences) and analyzed using FlowJo software (Tree Star, Ashland, OR). For intracellular cytokine staining, cells were fixed with 4% paraformaldehyde, permeabilized with 0.5% saponin, and stained with anti–DAP12-PE mAb along with proper isotype control.

Human osteoclast cultures and functional assessment of osteoclast formation

The University of California Davis Institutional Review Board committee approved all protocols. PBMCs were isolated from healthy volunteers by density-gradient centrifugation with Histopaque-1077 (Sigma-Aldrich, St. Louis, MO) as previously described (27). $CD14^+$ cells were isolated with the MACS monocyte isolation Kit (Miltenyi Biotec). PBMC or $CD14^+$ cells were added to 96-well tissue-culture plates containing dentine slices (prepared in-house) or coverslips (Electron Microscopy Sciences) as previously described (27). PBMC cultures were maintained in the presence of 30 ng/ml sRANKL and 25 ng/ml M-CSF as positive control or only M-CSF as a negative control. Functional assessment of osteoclast formation was performed using TRAP, F-actin, bone resorption assays, quantitative PCR, and scanning electron microscopy as previously described (27, 28).

Lentivirus transduction of DAP12 ITAM mutant forms

DAP12 ITAM mutant forms Y91F, Y102F, and Y91F/102F (2YF) were generated by site-directed mutagenesis (Stratagene), and clones were confirmed by sequencing. The majority of hematopoietic cells are nondividing or slowly self-renewing and thus refractory to most nonviral or retroviral delivery methods. Because lentiviral vectors are capable of transducing nondividing cells and maintaining long-term and sustained expression of the transgenes, we used an HIV-1–derived vector system with minor modifications (29). Human wild-type DAP12 and DAP12 mutants containing the Xpress peptide epitope (DLYDDDDK) were subcloned into the pCCLsin.PPT.hEF1a.pre vector (S. Gupta, Albert Einstein College of Medicine). The human alpha1-antitrypsin promoter was replaced with human elongation factor 1a promoter. To generate the retrovirus, HEK293T cells were cotransfected with pCCL constructs and packaging plasmids pMDLg/pRRE, pRSV-Rev, and pMD2.VSV-G using polyfect (Qiagen). Viral titers of 5×10^6 viral particles measured by QuickTiter Lentivirus Quantitation Kit (Cell Biolabs) were used for optimal infection. This viral titer had no cytotoxic effects on target cells. The virus-containing supernatant was collected 72 h after transfection and added to PBMCs plated on 10-cm culture dishes. After 48 h, the viral supernatant was replaced with fresh medium. Cells were stimulated with IL-23 as described above.

Western blotting and immunoprecipitation

Cytokine-treated PBMCs were washed two times with ice-cold Dulbecco's PBS and lysed with mammalian cell lysis buffer (50 mM Tris-HCl [pH 7.4], 150 mM NaCl, 1 mM EDTA, 1% Triton X-100, 1 mM PMSF, 1 mM sodium orthovanadate, and 1 mM sodium fluoride) by incubation on ice for 15 min. The cell lysates were clarified by centrifugation at 15,000 rpm for 10 min at 4˚C before being analyzed by Western blotting. For immunoprecipitation experiments, protein G-Dynabeads were incubated with the appropriate specific Ab for 1 h at 4˚C. Cell lysates were precleared with protein G-Dynabeads for 30 min at 4˚C and then incubated with the protein G-Dynabead–appropriate specific Ab complex for >2 h at 4˚C. After washing three times with wash buffer, immunoprecipitated protein lysates and whole cell lysates were separated by SDS-PAGE and transferred onto a polyvinylidene difluoride membrane. The membrane was probed with the appropriate primary Abs, followed by detection with HRP-conjugated secondary Ab, and detected by ECL reagent or Odyssey (Li-Cor).

Intracellular calcium measurements

PBMCs treated with M-CSF for 8 d and serum starved for 18 h were labeled with 3 μM Fluo-4 AM for 30 min at 37˚C prior to imaging. A total of 100 ng/ml IL-23 or 100 ng/ml RANKL was added after 5 min of baseline imaging, and calcium activity was tracked in the same cells over the next 10 min. For inhibition experiments, PBMCs expanded with M-CSF for 8 d were pretreated with 1 μM PLC inhibitor U73122 for 15 min prior to calcium imaging and stimulation with 100 ng/ml IL-23 or 100 ng/ml RANKL as before. Fluo-4 AM intensity per cell was measured and tracked over time using the Nikon NIS elements Br software (Nikon).

Statistical analysis

Data were analyzed using Mann–Whitney *U* test. One-way or two-way ANOVA with Bonferroni posttest was used where appropriate. A p value <0.05 was considered to be statistically significant (minimum $n = 3$).

Results

IL-23 induces osteoclast formation in human PBMC in a RANKL-independent manner

To study the direct effect of IL-23 in myeloid cells, human PBMC-adherent cells were cultured for 8 d in the presence of M-CSF. Exogenous IL-23 addition to M-CSF expanded PBMCs and stimulated the formation of large, $TRAP^+$, multinucleated cells in the absence of exogenous RANKL stimulation (Fig. 1A). These cells were capable of F-actin ring formation and bone resorption when placed on dentine slices (Fig. 1B, 1C). Although the percentage surface area of dentine resorption induced by IL-23 (16 ± 3%) was not significantly different from that of RANKL (22 ± 7%) (Fig. 1D), the resorption pits induced by IL-23 were shallower with no distinct edges and not as deep and defined as in RANKL-induced cultures. This observation is consistent with the resorption pits typically induced by TNF, IL-1, IL-6, IL-11, and other proinflammatory cytokines (27, 30). IL-23 effects were independent of RANKL, as addition of OPG was not as able to block the IL-23–induced osteoclastogenesis (Fig. 1D). However, in agreement with the synergistic effect of proinflammatory cytokines with RANKL, IL-23 induced an increase in bone resorption with RANKL (Fig. 1E).

Multianalyte analysis of conditioned medium from M-CSF–expanded PBMCs stimulated with increasing levels of IL-23 was performed to address the role of known IL-23–induced factors on the osteoclast precursors. Because IL-23 induces IL-17 from a number of cell types (31) and IL-17 influences osteoclast formation (32), we performed a dose response of IL-23 alone and in conjunction with RANKL in four individual donors and measured the amount of IL-17 in the conditioned medium (Supplemental Fig. 1). We also checked for the ex-

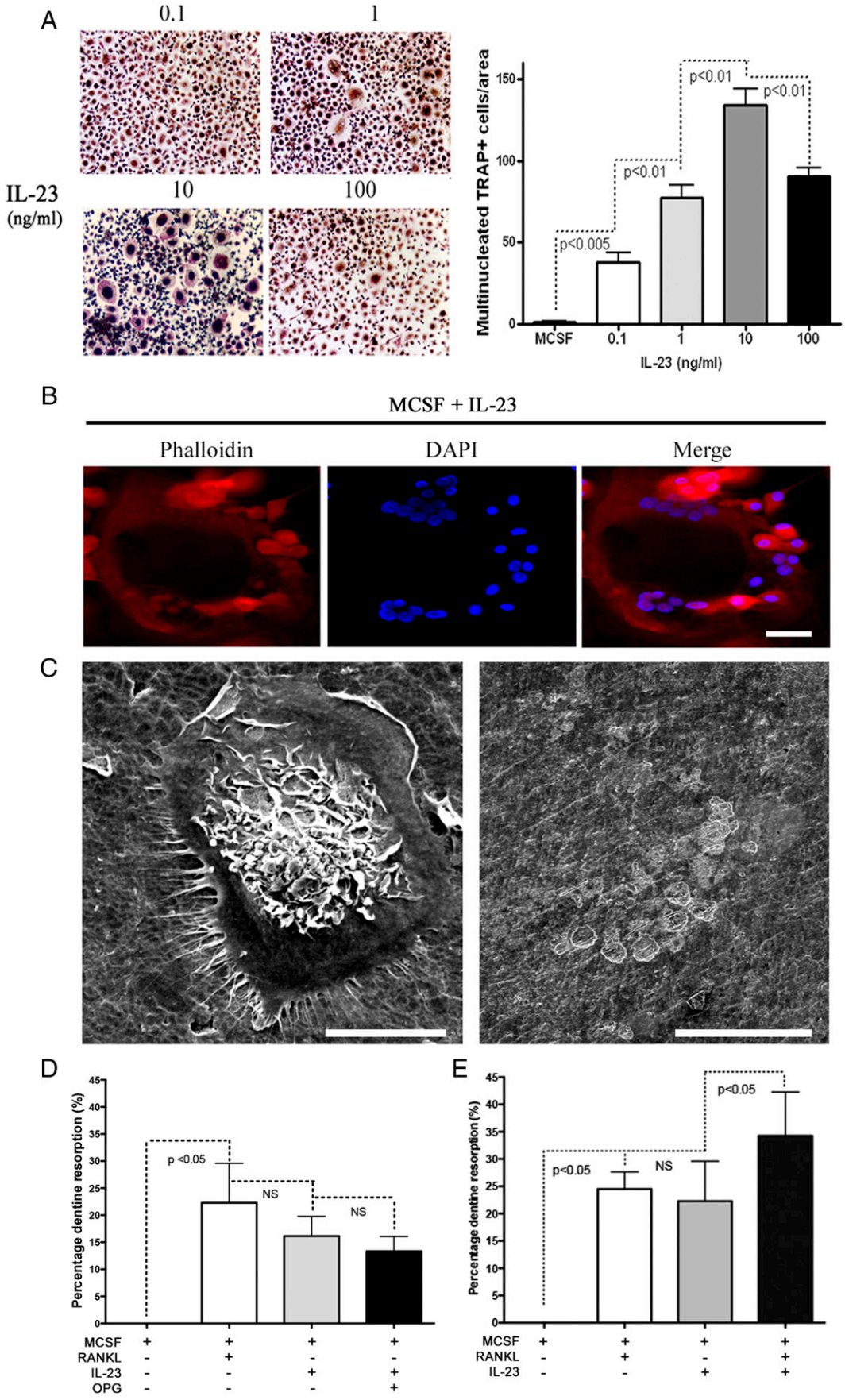

FIGURE 1. IL-23 induces human osteoclast formation in PBMCs in vitro. (**A**) TRAP staining of human PBMC isolated from healthy volunteers cultured for 14 d in the presence of M-CSF and increasing IL-23 concentrations. Original magnification ×100. Data pooled from four individual experiments done in triplicates. (**B**) Phalloidin and DAPI staining and merged image of both stains of PBMCs cultured on coverslips for 18 d in the (*Figure legend continues*)

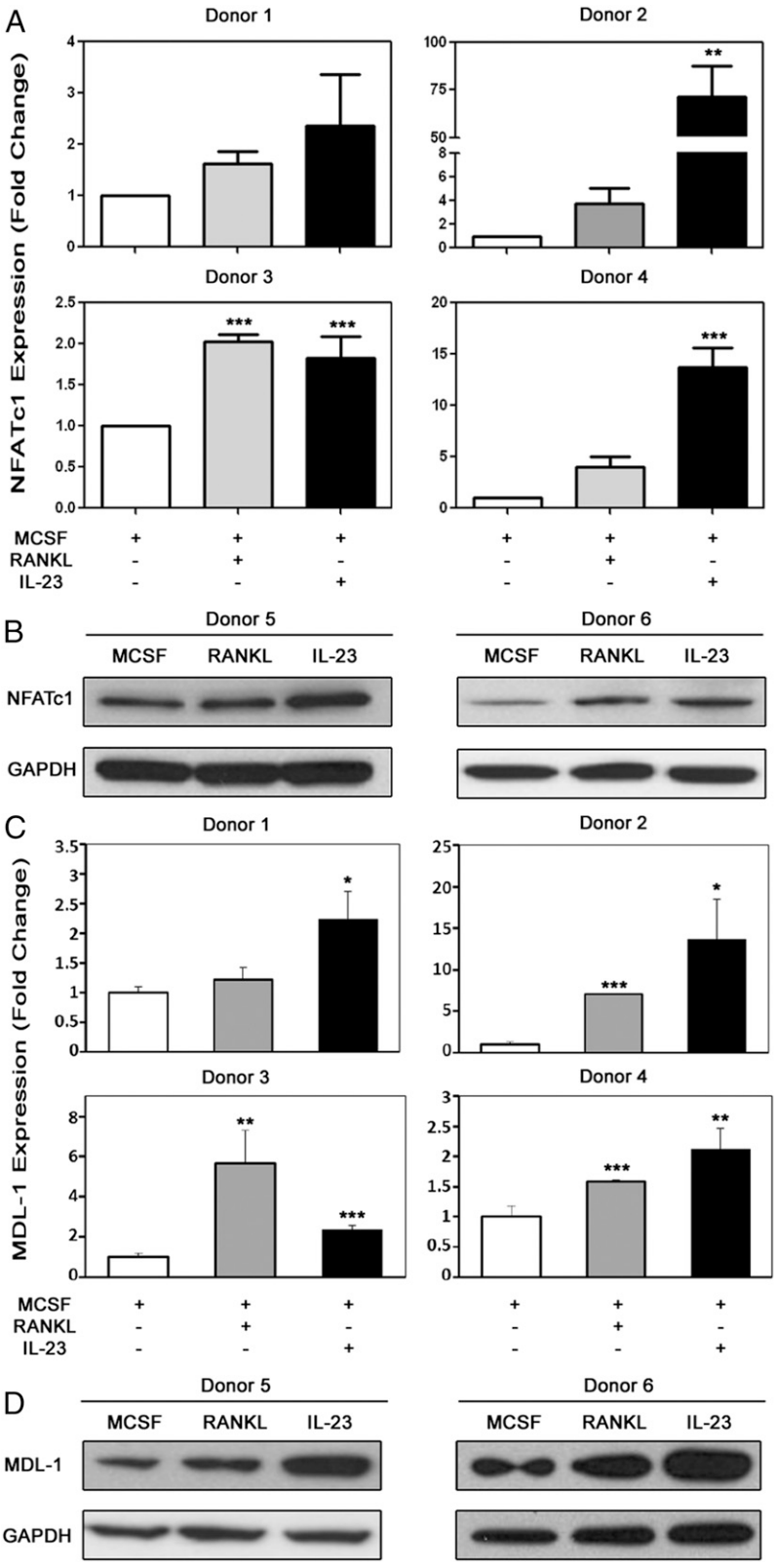

FIGURE 2. IL-23 induces expression of NFATc1 and MDL-1. Quantitative RT-PCR showing NFATc1 gene expression relative to 18S (**A**) and Western blotting showing NFATc1 protein expression relative to GAPDH (**B**) in PBMC 8-d cultures treated with M-CSF and/or RANKL and/or IL-23. Quantitative RT-PCR showing MDL-1 gene expression relative to 18S in PBMC 8 d cultures treated with M-CSF and/or RANKL (**C**) and/or IL-23 Western blotting showing MDL-1 protein expression relative to GAPDH in PBMC 8-d cultures treated with M-CSF and/or RANKL and/or IL-23 (**D**). Error bars represent the SD of the mean (*t* test, $*p < 0.05$, $**p < 0.01$, $***p < 0.001$).

presence of M-CSF and IL-23 showing F-actin ring formation. Scale bar, 25 μm. Representative of 20 independent experiments. (**C**) PBMC cultured on dentine slices for 18 d in the presence of M-CSF and IL-23 showing dentine erosion. Scale bars, 25 and 100 μm, *left* and *right panels*, respectively. Representative of 20 independent experiments. Mean percentage lacunar resorption in PBMC after treatment with M-CSF and sRANKL or M-CSF with IL-23 (± OPG) (**D**) or M-CSF and sRANKL or M-CSF with RANKL and IL-23 (**E**). Representative of six independent experiments. Error bars represent SE of the mean ($p < 0.05$). One-way ANOVA and *t* test were used where appropriate.

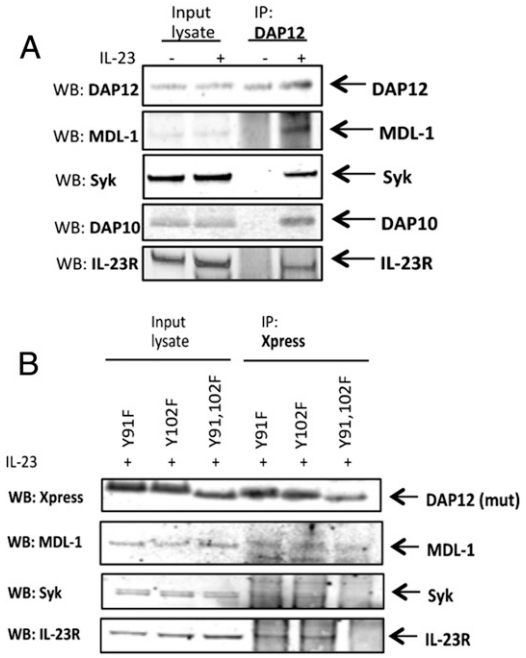

FIGURE 3. IL-23 elicits ITAM signaling through DAP12. (**A**) Total cell lysates of human PBMCs expanded for 8 d with M-CSF, serum starved, and stimulated with 100 ng/ml of IL-23 (+) or control medium (−) were immunoprecipitated (IP) with DAP12 Ab and immunoblotted with DAP12, MDL-1, Syk, DAP10, or IL-23R Abs. Representative of two independent experiments. (**B**) Total cell lysates of lentivirally transduced mutant forms of DAP12, Y91F, Y102F, Y91, and 102F (Y2F) expanded for 8 d with M-CSF serum starved and stimulated with 100 ng/ml of IL-23 (+) or control medium (−) were immunoprecipitated with DAP12 Ab and immunoblotted with DAP12, MDL-1, Syk, or IL-23R Abs. Representative of two independent experiments. WB, Western blot.

pression of the osteoclastogenic factors RANKL and TNF in PBMC conditioned medium, as they are also released from Th17 cells. The amount of the osteoclastogenic cytokines in the conditioned medium was at least 1000-fold below what is required to be biologically active (32) in our in vitro osteoclastogenesis assays, and furthermore, neutralizing Abs to IL-17 and TNF were not as able to block the IL-23–induced osteoclastogenesis. Taken together, these data confirm that IL-23 induces human osteoclast formation in human PBMCs in a Th17- and RANKL-independent manner.

IL-23 induces the upregulation of MDL-1 and NFATc1

PBMCs were isolated from healthy donors and expanded for 8 d in the presence of M-CSF (negative control), M-CSF + RANKL (positive control), or M-CSF + IL-23. IL-23 induced the upregulation of both NFATc1 message (Fig. 2A) and protein (Fig. 2B). Similarly, MDL-1 message (Fig. 2C) and protein levels (Fig. 2D) were also elevated upon stimulation by either IL-23 or RANKL. It is noteworthy that in certain donors, the upregulation of MDL-1 and NFATc1 by IL-23 equaled or even exceeded the induction by RANKL. Because both MDL-1 and NFATc1 have direct roles in osteoclastogenesis (33, 34), we investigated whether MDL-1 may lead to osteoclast activation following IL-23 signaling.

IL-23 induces the formation of an IL-23R/MDL-1/DAP12 complex

In osteoclast precursors, multiple immunoreceptors associate with DAP12 to stimulate NFATc1 induction and osteoclastogenesis (16, 23–26). Therefore, we investigated the interaction of MDL-1 with DAP12 in NFATc1 activation. DAP12 was immunoprecipitated from M-CSF–expanded human PBMCs stimulated with and without 100 ng/ml IL-23. Upon IL-23 stimulation, DAP12 formed a complex with MDL-1, DAP10, the IL-23R, and SYK (Fig. 3A). We expressed various N-terminal Xpress-tagged DAP12 mutants using a lentiviral system to investigate the role of DAP12's ITAM in the immunocomplex. Specifically, the Y91F, Y102F (single mutants), and Y91F/Y102F (2YF double-mutant) DAP12 mutants contained tyrosine to phenylalanine

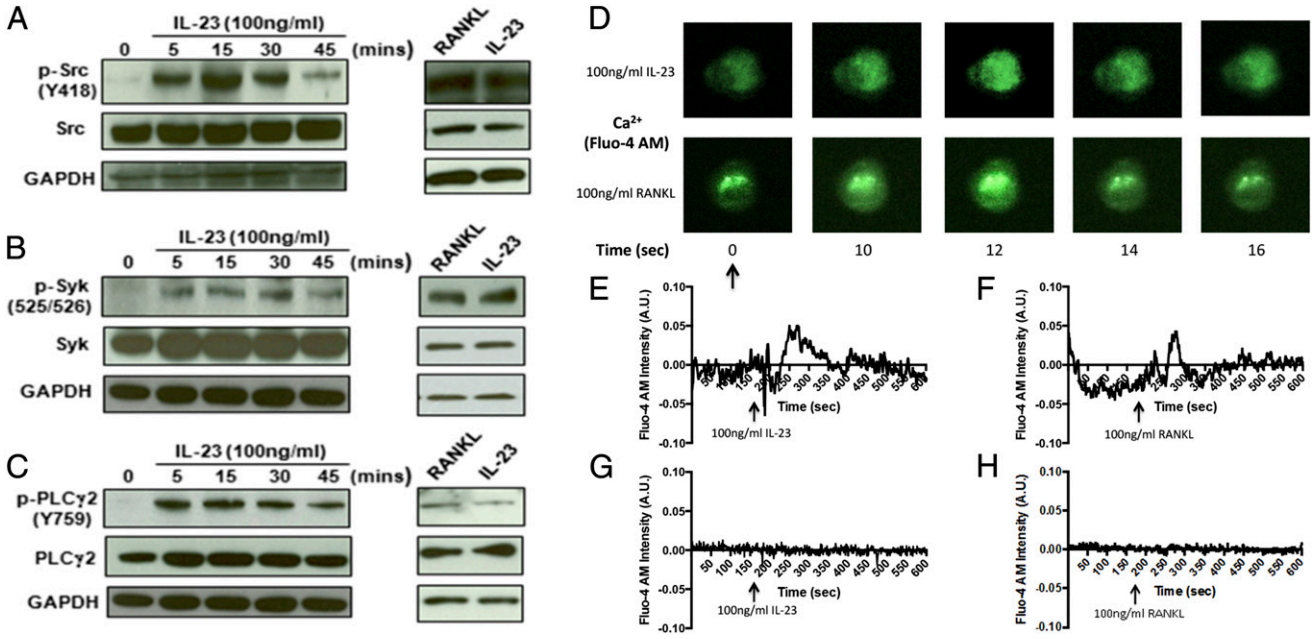

FIGURE 4. IL-23 activates PLCγ-mediated calcium flux in osteoclast precursors. Western blotting of human PBMCs expanded with M-CSF for 8 d, serum starved for 18 h, stimulated with 100 ng/ml of M-CSF, RANKL, or IL-23 for indicated time, and probed with anti-phosphotyrosine Src (Y418) and total Src (**A**), anti-phosphotyrosine Syk (Y525/526) and total Syk (**B**), and anti-phosphotyrosine PLCγ2 (Y759) and total PLCγ2 (**C**). *Right panels* show comparative phosphorylation using 10 ng/ml of IL-23 and 30 ng/ml of RANKL at 5-min time point. (**D**) Calcium imaging intensity in human PBMCs expanded with M-CSF for 8 d, serum starved for 18 h, labeled with 3 μM Fluo-4 AM (original magnification ×200), and stimulated with 100 ng/ml of IL-23 (**E**) or RANKL (**F**) for indicated times. (**G** and **H**) Same conditions as (E) and (F) but with prior incubation with protein kinase C inhibitor before IL-23 or RANKL stimulation. Fluo-4 AM intensity was measured and normalized per cell. Representative images and curves of cells exhibiting calcium flux are shown. Representative of four independent experiments. A.U., arbitrary units.

mutations to address the reduced or complete inhibition of DAP12 ITAM phosphorylation. IL-23 stimulation of DAP12 mutant–transduced PBMCs resulted in the absence of IL-23R and SYK recruitment (Fig. 3B). The association of MDL-1 with DAP12 was not so dramatically affected, confirming previous observations that DAP12 pairs with MDL-1 in unstimulated cells.

IL-23 activates SRC, SYK, and PLCγ2 phosphorylation and induces calcium transients

Next, we stimulated osteoclast precursors with 100 ng/ml IL-23 to investigate the time-dependent activation of NFATc1 by IL-23. IL-23 induced a rapid (within 5 min) phosphorylation of SRC (Y418), SYK (Y525/526), and PLCγ2 (Y759) (Fig. 4A–C). We next compared IL-23's signal strength to RANKL at the concentrations used in the osteoclastogenesis cultures (i.e., 10 and 30 ng/ml, respectively). At 5 min, IL-23–induced SRC and SYK phosphorylation was comparable to RANKL's activity; however, PLCγ2 phosphorylation was slightly reduced in comparison with RANKL's effect (Fig. 4A–C). We next investigated whether IL-23–induced phosphorylation lead to an increase in cytosolic calcium. IL-23 stimulation of M-CSF–expanded PBMCs showed an immediate increase in calcium flux within 10 s as detected by Fluo-4 AM (Fig. 4D), with the calcium flux intensity being comparable to RANKL's calcium flux (Fig. 4E, 4F). Addition of 1 μM PLCγ inhibitor U73122 15 min prior to calcium measurements and stimulation with 100 ng/μl IL-23 or RANKL completely inhibited IL-23– or RANKL-induced calcium flux (Fig. 4G, 4H).

IL-23 activates nuclear NFATc1 and initiates transcription of osteoclast-specific genes

IL-23 induced the translocation of NFATc1 to the nucleus and induced NFATc1 activity to similar levels as RANKL (Fig. 5A, 5B). We next investigated the IL-23 induction of a number of osteoclast-associated genes that were regulated by NFATc1 at 8 and 18 d of culture. IL-23 induced the expression of TRAP, matrix metallopeptidase 9 (MMP9), and calcitonin receptor in the absence of exogenous RANKL (Fig. 5C–E). Cathepsin K, however, was not modulated by IL-23. Furthermore, NFATc1 and other osteoclast-related genes were also modulated by IL-23 in a dose-response manner in synergy with RANKL (Supplemental Fig. 2).

MDL-1–expressing cells are enriched in the promyelocytes

Next, we sorted the $CD14^+$ fraction of the PBMCs and stimulated with M-CSF + IL-23. Although IL-23 in the presence of M-CSF

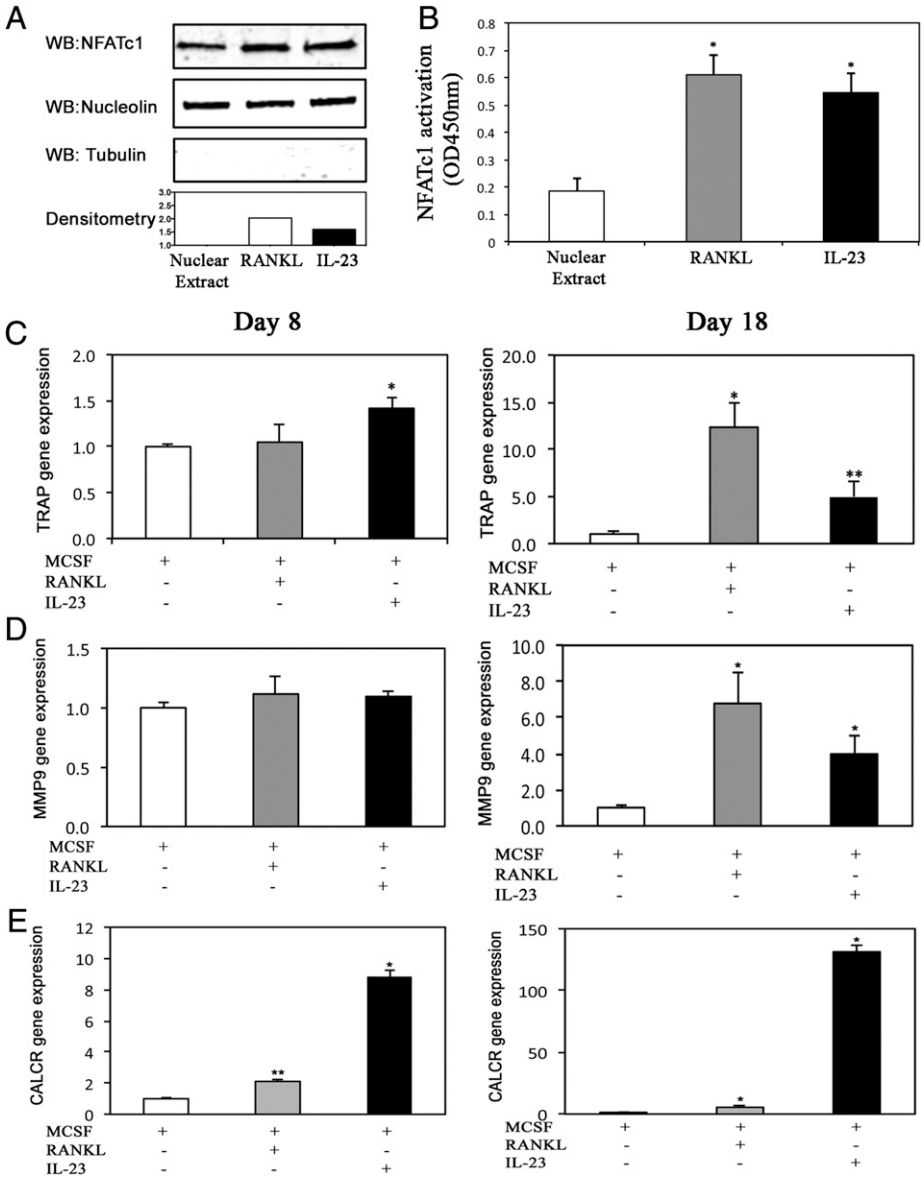

FIGURE 5. IL-23 induces NFATc1-dependent activation of osteoclast-associated genes. (**A**) Nuclear extracts of human PBMCs treated with M-CSF for 8 d, serum starved for 18 h, and stimulated with 100 ng/ml of IL-23 or RANKL. Extracts were probed with NFATc1, nucleolin, and tubulin Abs, and densitometry measurements quantified NFATc1 nuclear translocation. (**B**) NFATc1 activation was measured using a TransAM NFATc1 assay kit. Quantitative RT-PCR analysis showing (**C**) TRAP, (**D**) MMP9, and (**E**) calcitonin receptor (CALCR) gene expression relative to 18S after 8 or 18 d treatment with M-CSF, or M-CSF + RANKL, or M-CSF + IL-23. Representative of four independent experiments. $*p < 0.05$, $**p < 0.01$. WB, Western blot.

induced the formation of multinucleated TRAP$^+$ cells, these cells were not capable of forming F-actin rings or resorbing dentine and therefore could not be characterized as functional osteoclasts (Fig. 6A, 6B). Surprisingly, IL-23 did not induce osteoclast formation in the CD14$^+$ fraction of PBMCs, suggesting that this novel pathway may use a different cell precursor. We also observed that the expression of MDL-1 was almost absent in the CD14$^+$ fraction of PBMCs. Flow cytometric analysis of PBMCs by gating on MDL-1$^{+/}$DAP12$^+$ cells revealed that the expression of MDL-1$^{+/}$DAP12$^+$ was largely confined within the CD16$^+$ myeloid population (Fig. 6C).

Discussion

In this paper, we describe a direct mechanism of IL-23 in macrophage activation. Specifically, our data have highlighted that human macrophages respond to IL-23 with a strong upregulation of MDL-1, a PU.1 transcriptional target during myeloid differentiation (35). MDL-1 was recently identified to play a major role in myeloid progenitors, capable of osteoclast formation in inflammatory arthritis (33, 36). As DAP12 interacts with MDL-1, we explored the IL-23–elicited responses within the MDL-1/DAP12 pathway. We found that DAP12 associates with MDL-1 and DAP10 following IL-23 stimulation. Furthermore, this interaction induces SRC phosphorylation, which recruits SYK and phosphorylates effectors and transducers of calcium signaling including PLCγ2, which regulates osteoclastogenesis (37). IL-12, which shares IL-12/23p40 and IL-12Rβ1 with IL-23, regulates many classes of ITAM-bearing receptors in NK and T cells through synergy with DAP10, resulting in potent costimulatory signals (38, 39). Although DAP10 was previously shown to form an MDL-1–DAP12/DAP10 trimolecular complex, which triggers osteoclastogenesis, the interactions with IL-23 have not been described previously (40).

Our data revealed that ITAMs are critical for the recruitment of SYK, PLCγ2 phosphorylation, and generation of intracellular calcium after IL-23 signaling. A link between proinflammatory cytokines and Ca^{2+} signaling has previously been described through TNF, which induces Ca^{2+} oscillations in human macrophages and leads to activation of NFATc1 (41). Although IL-23 did not induce Ca^{2+} oscillations but Ca^{2+} transients (irregular oscillations), it was still able to induce NFATc1, suggesting that Ca^{2+} oscillations are not required in IL-23–induced dephosphorylation of the Ca^{2+}-dependent phosphatase calcineurin and subsequent induction of NFATc1. In myeloid cells where basal NFAT expression is low, the initiation of osteoclast differentiation requires the induction of NFATc1 expression. IL-23 induces the molecular machinery to orchestrate upregulation of cytoplasmic NFATc1. Furthermore, we show that IL-23 induces the subsequent translocation of NFATc1 to the nucleus, and the initiation of transcription of NFATc1 target genes such as TRAP, MMP9, CTSK, ITGB3, and CLCN7 further amplifies osteoclastogenesis (42). It is also noteworthy that the effects of IL-23 were directly compared with RANKL, which is the most potent osteoclastogenic factor in vivo and in vitro, and in most cases, the effects of IL-23 were greater than RANKL. However, IL-23 did not induce the upregulation of CTSK, and this may account for the impaired dentine degradation observed in dentine discs compared with RANKL. This may be due to the fact that IL-23 regulates IFN, which is known to downregulate cathepsin K gene expression (43).

Another striking difference between RANKL and IL-23 signaling derived from the phenotypic analysis of the myeloid cells involved in NFATc1 activation. RANK receptor is predominantly expressed in the CD14$^+$ fraction of PBMCs, and much of the published literature regarding osteoclastogenesis has used CD14$^+$ as an osteoclast precursor in in vitro assays (44). Surprisingly, sorted CD14$^+$ cells that were stimulated with IL-23 did not produce any functional osteoclasts, although they did induce cell fusion.

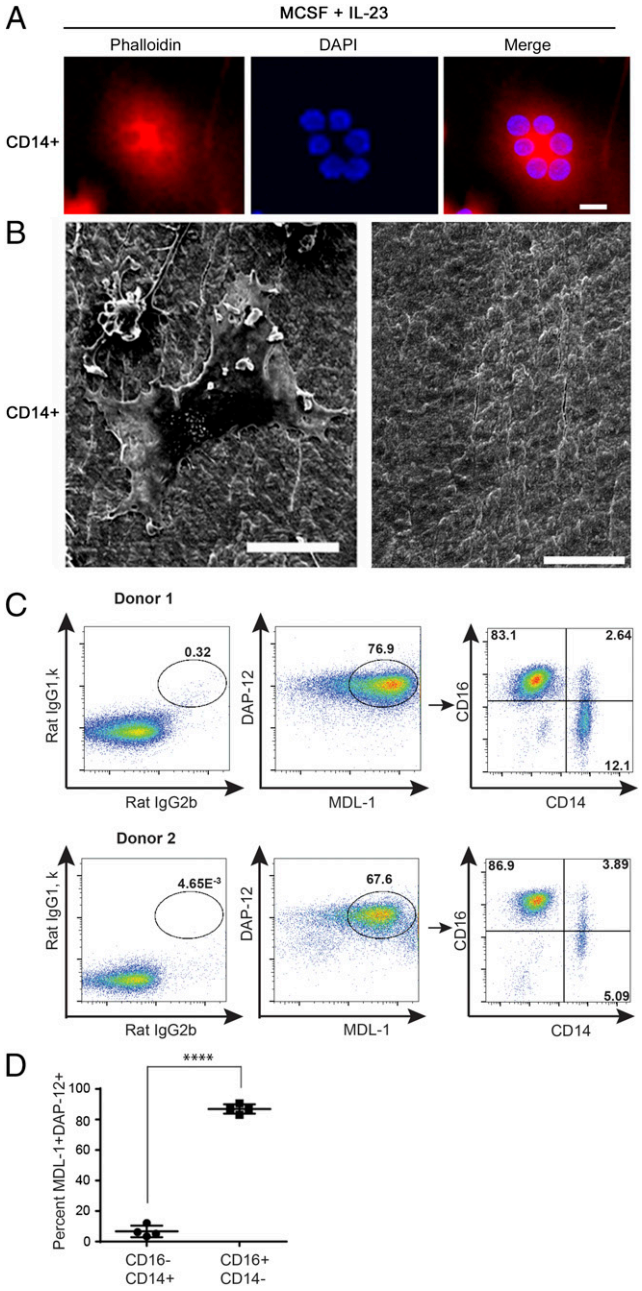

FIGURE 6. IL-23 does not induce osteoclast differentiation in the CD14$^+$ fraction of PBMC. (**A**) Phalloidin and DAPI staining and merged image of both stains of the CD14$^+$ fraction of human PBMCs cultured on coverslips for 18 d in the presence of M-CSF and IL-23 showing multinucleation but no F-actin ring formation. Scale bar, 25 μm. (**B**) CD14$^+$ fraction of human PBMCs cultured on dentine slices for 18 d in the presence of M-CSF and IL-23 showing absence of dentine erosion. Scale bars, 25 and 100 μm, *left* and *right panels*, respectively. (**C**) Representative data from flow cytometric analysis of two donors showing the expression of CD16 and CD14 in MDL-1$^+$/DAP12$^+$ double-positive gated populations of the PBMC fraction. The forward scatter and side scatter gating strategy excluded the debris, doublets, dead cells, and the majority of the lymphocyte fraction. (**D**) Graphical representation showing the mean percentage ± SEM of MDL-1$^+$DAP12$^+$ cells in CD14 and CD16 subsets of healthy donors (n = 4, solid line represents the mean; ****$p < 0.0001$).

Similar observations in which IL-23 failed to induce osteoclast formation in $CD14^+$ have previously been reported, but no mechanism was proposed (45). Other studies have also shown that IL-23 induces osteoclast formation, but again no mechanism has been proposed (46). Phenotypic analysis of various PBMC fractions by flow cytometry revealed that the double-positive $MDL\text{-}1^+/DAP12^+$ cells are within the $CD16^+$ fraction of PBMCs. Therefore, IL-23 activates a different subset of myeloid progenitor cells than RANKL and induces their differentiation to osteoclasts. This is of particular importance, as in inflammatory arthritis, a combination of IL-23 and RANKL will have an additive and more bone-destructive effect because it uses different osteoclast precursors while at the same time inducing a costimulatory pathway. This explains why we see an increased induction of RANKL-induced osteoclastogenesis and further increase bone resorption in vitro, which correlated with an increase in osteoclast-associated mRNA for NFATc1, TRAF6, TRAP, CTNN, and ITGB3 in a dose-dependent manner. It also points to the possibility that different cell subsets of monocytes and macrophages may get activated by proinflammatory cytokines to differentiate to osteoclasts in inflammatory arthritis, which are completely different from those regulated by RANKL during physiological bone remodeling.

The data described in this paper are independent of the Th17 effects on osteoclast differentiation (15). IL-17 was barely detectable in IL-23–stimulated PBMC supernatants, and the IL-17 concentrations were much lower than are needed to directly promote osteoclastogenesis using this assay system (32). A report by Chen et al. (47) showed that IL-23 upregulated RANK in RAW 264.7 cells; however, in our studies with human PBMCs, there was no detectable elevation of RANK protein by flow cytometry even after 18 d of IL-23 stimulation. Our data show that IL-23 acts on human $CD16^+$ $MDL\text{-}1^{+/}DAP12^+$ osteoclast precursor population to induce osteoclast differentiation. This novel pathway uses the DAP12 ITAMs to recruit SYK and induce Ca^{2+}-dependent activation of NFATc1. Collectively, our data define a novel pathway that is used by IL-23 in myeloid cells and identify a major mechanism for the stimulation of osteoclastogenesis.

Disclosures

E.P.B. is an employee of Merck.

References

1. Dale, D. C., L. Boxer, and W. C. Liles. 2008. The phagocytes: neutrophils and monocytes. *Blood* 112: 935–945.
2. Wynn, T. A., A. Chawla, and J. W. Pollard. 2013. Macrophage biology in development, homeostasis and disease. *Nature* 496: 445–455.
3. Hume, D. A., and K. P. MacDonald. 2012. Therapeutic applications of macrophage colony-stimulating factor-1 (CSF-1) and antagonists of CSF-1 receptor (CSF-1R) signaling. *Blood* 119: 1810–1820.
4. Sarma, U., and A. M. Flanagan. 1996. Macrophage colony-stimulating factor induces substantial osteoclast generation and bone resorption in human bone marrow cultures. *Blood* 88: 2531–2540.
5. Fujikawa, Y., J. M. Quinn, A. Sabokbar, J. O. McGee, and N. A. Athanasou. 1996. The human osteoclast precursor circulates in the monocyte fraction. *Endocrinology* 137: 4058–4060.
6. Lacey, D. L., E. Timms, H. L. Tan, M. J. Kelley, C. R. Dunstan, T. Burgess, R. Elliott, A. Colombero, G. Elliott, S. Scully, et al. 1998. Osteoprotegerin ligand is a cytokine that regulates osteoclast differentiation and activation. *Cell* 93: 165–176.
7. Schwarzenberger, P., V. La Russa, A. Miller, P. Ye, W. Huang, A. Zieske, S. Nelson, G. J. Bagby, D. Stoltz, R. L. Mynatt, et al. 1998. IL-17 stimulates granulopoiesis in mice: use of an alternate, novel gene therapy-derived method for in vivo evaluation of cytokines. *J. Immunol.* 161: 6383–6389.
8. Pelletier, M., L. Maggi, A. Micheletti, E. Lazzeri, N. Tamassia, C. Costantini, L. Cosmi, C. Lunardi, F. Annunziato, S. Romagnani, and M. A. Cassatella. 2010. Evidence for a cross-talk between human neutrophils and Th17 cells. *Blood* 115: 335–343.
9. Liu, B., W. Tan, A. Barsoum, X. Gu, K. Chen, W. Huang, A. Ramsay, J. K. Kolls, and P. Schwarzenberger. 2010. IL-17 is a potent synergistic factor with GM-CSF in mice in stimulating myelopoiesis, dendritic cell expansion, proliferation, and functional enhancement. *Exper. Hematol.* 38: 877–884.e871.
10. Langrish, C. L., Y. Chen, W. M. Blumenschein, J. Mattson, B. Basham, J. D. Sedgwick, T. McClanahan, R. A. Kastelein, and D. J. Cua. 2005. IL-23 drives a pathogenic T cell population that induces autoimmune inflammation. *J. Exp. Med.* 201: 233–240.
11. Adamopoulos, I. E., M. Tessmer, C. C. Chao, S. Adda, D. Gorman, M. Petro, C. C. Chou, R. H. Pierce, W. Yao, N. E. Lane, et al. 2011. IL-23 is critical for induction of arthritis, osteoclast formation, and maintenance of bone mass. *J. Immunol.* 187: 951–959.
12. Parham, C., M. Chirica, J. Timans, E. Vaisberg, M. Travis, J. Cheung, S. Pflanz, R. Zhang, K. P. Singh, F. Vega, et al. 2002. A receptor for the heterodimeric cytokine IL-23 is composed of IL-12Rbeta1 and a novel cytokine receptor subunit, IL-23R. *J. Immunol.* 168: 5699–5708.
13. Verreck, F. A., T. de Boer, D. M. Langenberg, M. A. Hoeve, M. Kramer, E. Vaisberg, R. Kastelein, A. Kolk, R. de Waal-Malefyt, and T. H. Ottenhoff. 2004. Human IL-23-producing type 1 macrophages promote but IL-10-producing type 2 macrophages subvert immunity to (myco)bacteria. *Proc. Natl. Acad. Sci. USA* 101: 4560–4565.
14. Awasthi, A., L. Riol-Blanco, A. Jäger, T. Korn, C. Pot, G. Galileos, E. Bettelli, V. K. Kuchroo, and M. Oukka. 2009. Cutting edge: IL-23 receptor gfp reporter mice reveal distinct populations of IL-17-producing cells. *J. Immunol.* 182: 5904–5908.
15. Sato, K., A. Suematsu, K. Okamoto, A. Yamaguchi, Y. Morishita, Y. Kadono, S. Tanaka, T. Kodama, S. Akira, Y. Iwakura, et al. 2006. Th17 functions as an osteoclastogenic helper T cell subset that links T cell activation and bone destruction. *J. Exp. Med.* 203: 2673–2682.
16. Koga, T., M. Inui, K. Inoue, S. Kim, A. Suematsu, E. Kobayashi, T. Iwata, H. Ohnishi, T. Matozaki, T. Kodama, et al. 2004. Costimulatory signals mediated by the ITAM motif cooperate with RANKL for bone homeostasis. *Nature* 428: 758–763.
17. Kaifu, T., J. Nakahara, M. Inui, K. Mishima, T. Momiyama, M. Kaji, A. Sugahara, H. Koito, A. Ujike-Asai, A. Nakamura, et al. 2003. Osteopetrosis and thalamic hypomyelinosis with synaptic degeneration in DAP12-deficient mice. *J. Clin. Invest.* 111: 323–332.
18. Bakker, A. B., E. Baker, G. R. Sutherland, J. H. Phillips, and L. L. Lanier. 1999. Myeloid DAP12-associating lectin (MDL)-1 is a cell surface receptor involved in the activation of myeloid cells. *Proc. Natl. Acad. Sci. USA* 96: 9792–9796.
19. Ivashkiv, L. B. 2008. A signal-switch hypothesis for cross-regulation of cytokine and TLR signalling pathways. *Nat. Rev. Immunol.* 8: 816–822.
20. Wang, L., I. Tassiulas, K. H. Park-Min, A. C. Reid, H. Gil-Henn, J. Schlessinger, R. Baron, J. J. Zhang, and L. B. Ivashkiv. 2008. 'Tuning' of type I interferon-induced Jak-STAT1 signaling by calcium-dependent kinases in macrophages. *Nat. Immunol.* 9: 186–193.
21. Mócsai, A., M. B. Humphrey, J. A. Van Ziffle, Y. Hu, A. Burghardt, S. C. Spusta, S. Majumdar, L. L. Lanier, C. A. Lowell, and M. C. Nakamura. 2004. The immunomodulatory adapter proteins DAP12 and Fc receptor gamma-chain (FcRgamma) regulate development of functional osteoclasts through the Syk tyrosine kinase. *Proc. Natl. Acad. Sci. USA* 101: 6158–6163.
22. Lanier, L. L., and A. B. Bakker. 2000. The ITAM-bearing transmembrane adaptor DAP12 in lymphoid and myeloid cell function. *Immunol. Today* 21: 611–614.
23. Colonna, M. 2003. TREMs in the immune system and beyond. *Nat. Rev. Immunol.* 3: 445–453.
24. Humphrey, M. B., K. Ogasawara, W. Yao, S. C. Spusta, M. R. Daws, N. E. Lane, L. L. Lanier, and M. C. Nakamura. 2004. The signaling adapter protein DAP12 regulates multinucleation during osteoclast development. *J. Bone Miner. Res.* 19: 224–234.
25. Zou, W., H. Kitaura, J. Reeve, F. Long, V. L. Tybulewicz, S. J. Shattil, M. H. Ginsberg, F. P. Ross, and S. L. Teitelbaum. 2007. Syk, c-Src, the alphavbeta3 integrin, and ITAM immunoreceptors, in concert, regulate osteoclastic bone resorption. *J. Cell Biol.* 176: 877–888.
26. Zou, W., J. L. Reeve, Y. Liu, S. L. Teitelbaum, and F. P. Ross. 2008. DAP12 couples c-Fms activation to the osteoclast cytoskeleton by recruitment of Syk. *Mol. Cell* 31: 422–431.
27. Adamopoulos, I. E., A. Sabokbar, B. P. Wordsworth, A. Carr, D. J. Ferguson, and N. A. Athanasou. 2006. Synovial fluid macrophages are capable of osteoclast formation and resorption. *J. Pathol.* 208: 35–43.
28. Nesbitt, S. A., and M. A. Horton. 1997. Trafficking of matrix collagens through bone-resorbing osteoclasts. *Science* 276: 266–269.
29. Follenzi, A., and L. Naldini. 2002. Generation of HIV-1 derived lentiviral vectors. *Methods Enzymol.* 346: 454–465.
30. Kudo, O., A. Sabokbar, A. Pocock, I. Itonaga, Y. Fujikawa, and N. A. Athanasou. 2003. Interleukin-6 and interleukin-11 support human osteoclast formation by a RANKL-independent mechanism. *Bone* 32: 1–7.
31. Cua, D. J., and C. M. Tato. 2010. Innate IL-17-producing cells: the sentinels of the immune system. *Nat. Rev. Immunol.* 10: 479–489.
32. Adamopoulos, I. E., C. C. Chao, R. Geissler, D. Laface, W. Blumenschein, Y. Iwakura, T. McClanahan, and E. P. Bowman. 2010. Interleukin-17A upregulates receptor activator of NF-kappaB on osteoclast precursors. *Arthritis Res. Ther.* 12: R29.
33. Joyce-Shaikh, B., M. E. Bigler, C. C. Chao, E. E. Murphy, W. M. Blumenschein, I. E. Adamopoulos, P. G. Heyworth, S. Antonenko, E. P. Bowman, T. K. McClanahan, et al. 2010. Myeloid DAP12-associating lectin (MDL)-1 regulates synovial inflammation and bone erosion associated with autoimmune arthritis. *J. Exp. Med.* 207: 579–589.

34. Takayanagi, H., S. Kim, T. Koga, H. Nishina, M. Isshiki, H. Yoshida, A. Saiura, M. Isobe, T. Yokochi, J. Inoue, et al. 2002. Induction and activation of the transcription factor NFATc1 (NFAT2) integrate RANKL signaling in terminal differentiation of osteoclasts. *Dev. Cell* 3: 889–901.
35. Batliner, J., M. M. Mancarelli, M. Jenal, V. A. Reddy, M. F. Fey, B. E. Torbett, and M. P. Tschan. 2011. CLEC5A (MDL-1) is a novel PU.1 transcriptional target during myeloid differentiation. *Mol. Immunol.* 48: 714–719.
36. Charles, J. F., L. Y. Hsu, E. C. Niemi, A. Weiss, A. O. Aliprantis, and M. C. Nakamura. 2012. Inflammatory arthritis increases mouse osteoclast precursors with myeloid suppressor function. *J. Clin. Invest.* 122: 4592–4605.
37. Mao, D., H. Epple, B. Uthgenannt, D. V. Novack, and R. Faccio. 2006. PLCgamma2 regulates osteoclastogenesis via its interaction with ITAM proteins and GAB2. *J. Clin. Invest.* 116: 2869–2879.
38. Ortaldo, J. R., R. Winkler-Pickett, J. Wigginton, M. Horner, E. W. Bere, A. T. Mason, N. Bhat, J. Cherry, M. Sanford, D. L. Hodge, and H. A. Young. 2006. Regulation of ITAM-positive receptors: role of IL-12 and IL-18. *Blood* 107: 1468–1475.
39. Colucci, F. 2007. Unexpected partnership between IL-15 and DAP10. *Nat. Immunol.* 8: 1289–1291.
40. Inui, M., Y. Kikuchi, N. Aoki, S. Endo, T. Maeda, A. Sugahara-Tobinai, S. Fujimura, A. Nakamura, A. Kumanogoh, M. Colonna, and T. Takai. 2009. Signal adaptor DAP10 associates with MDL-1 and triggers osteoclastogenesis in cooperation with DAP12. *Proc. Natl. Acad. Sci. USA* 106: 4816–4821.
41. Yarilina, A., K. Xu, J. Chen, and L. B. Ivashkiv. 2011. TNF activates calcium-nuclear factor of activated T cells (NFAT)c1 signaling pathways in human macrophages. *Proc. Natl. Acad. Sci. USA* 108: 1573–1578.
42. Aliprantis, A. O., Y. Ueki, R. Sulyanto, A. Park, K. S. Sigrist, S. M. Sharma, M. C. Ostrowski, B. R. Olsen, and L. H. Glimcher. 2008. NFATc1 in mice represses osteoprotegerin during osteoclastogenesis and dissociates systemic osteopenia from inflammation in cherubism. *J. Clin. Invest.* 118: 3775–3789.
43. Kamolmatyakul, S., W. Chen, and Y. P. Li. 2001. Interferon-gamma down-regulates gene expression of cathepsin K in osteoclasts and inhibits osteoclast formation. *J. Dent. Res.* 80: 351–355.
44. Atkins, G. J., P. Kostakis, C. Vincent, A. N. Farrugia, J. P. Houchins, D. M. Findlay, A. Evdokiou, and A. C. Zannettino. 2006. RANK Expression as a cell surface marker of human osteoclast precursors in peripheral blood, bone marrow, and giant cell tumors of bone. *J. Bone Miner. Res.* 21: 1339–1349.
45. Yago, T., Y. Nanke, M. Kawamoto, T. Furuya, T. Kobashigawa, N. Kamatani, and S. Kotake. 2007. IL-23 induces human osteoclastogenesis via IL-17 in vitro, and anti-IL-23 antibody attenuates collagen-induced arthritis in rats. *Arthritis Res. Ther.* 9: R96.
46. Moon, S. J., I. E. Ahn, H. Jung, H. Yi, J. Kim, Y. Kim, S. K. Kwok, K. S. Park, J. K. Min, S. H. Park, et al. 2013. Temporal differential effects of proinflammatory cytokines on osteoclastogenesis. *Int. J. Mol. Med.* 31: 769–777.
47. Chen, L., X. Q. Wei, B. Evans, W. Jiang, and D. Aeschlimann. 2008. IL-23 promotes osteoclast formation by up-regulation of receptor activator of NF-kappaB (RANK) expression in myeloid precursor cells. *Eur. J. Immunol.* 38: 2845–2854.

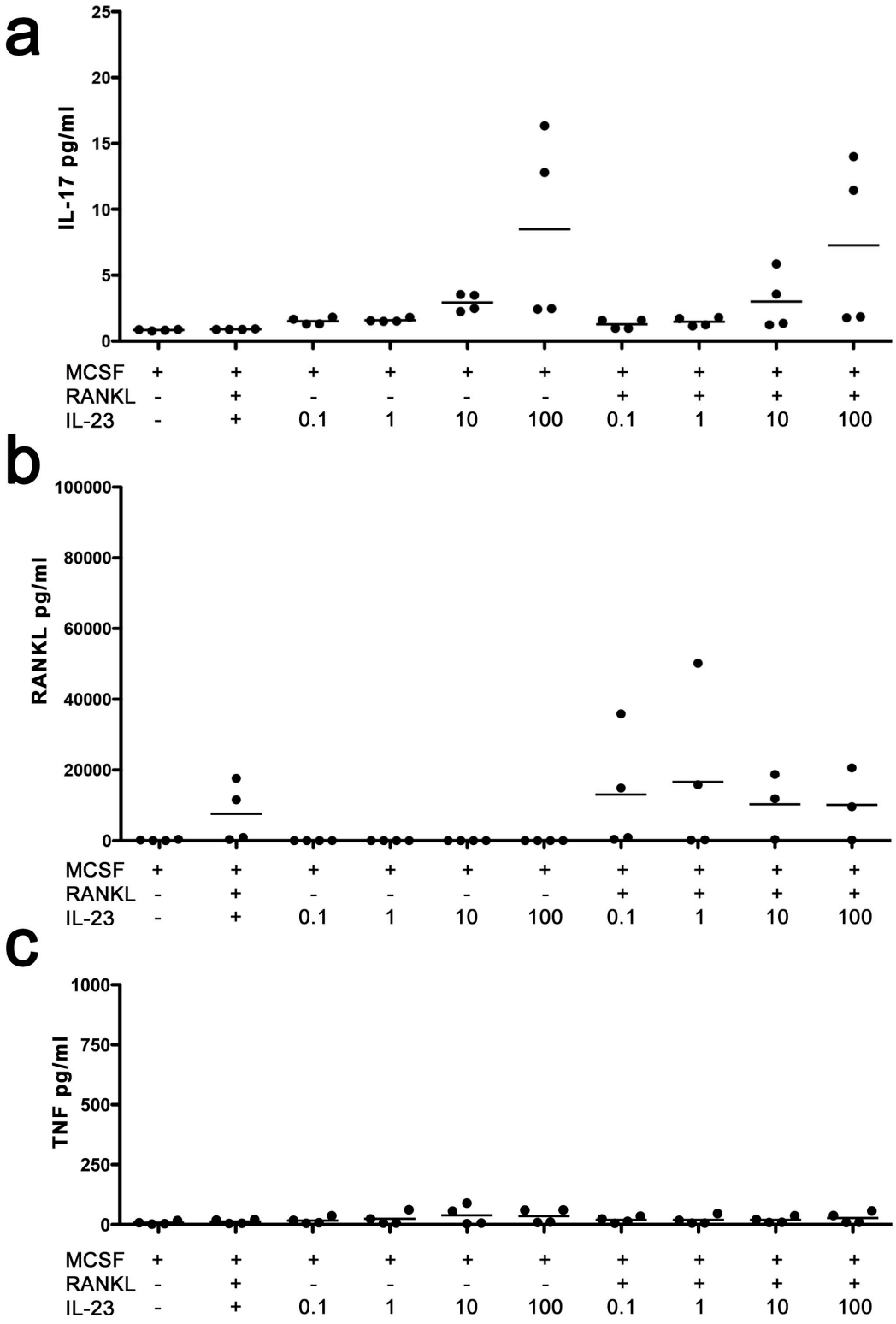

Supplementary Figure 1. IL-23 does not induce IL-17, RANKL or TNF secretion. Luminex analysis of **a)** IL-17A, **b)** RANKL, and **c)** TNF concentrations of PBMC conditioned medium cultured with increasing doses of IL-23 (0.1, 1, 10 or 100 ng/ml) in the absence or presence of RANKL (30ng/ml). (Each dot is a single donor; 4 donors total).

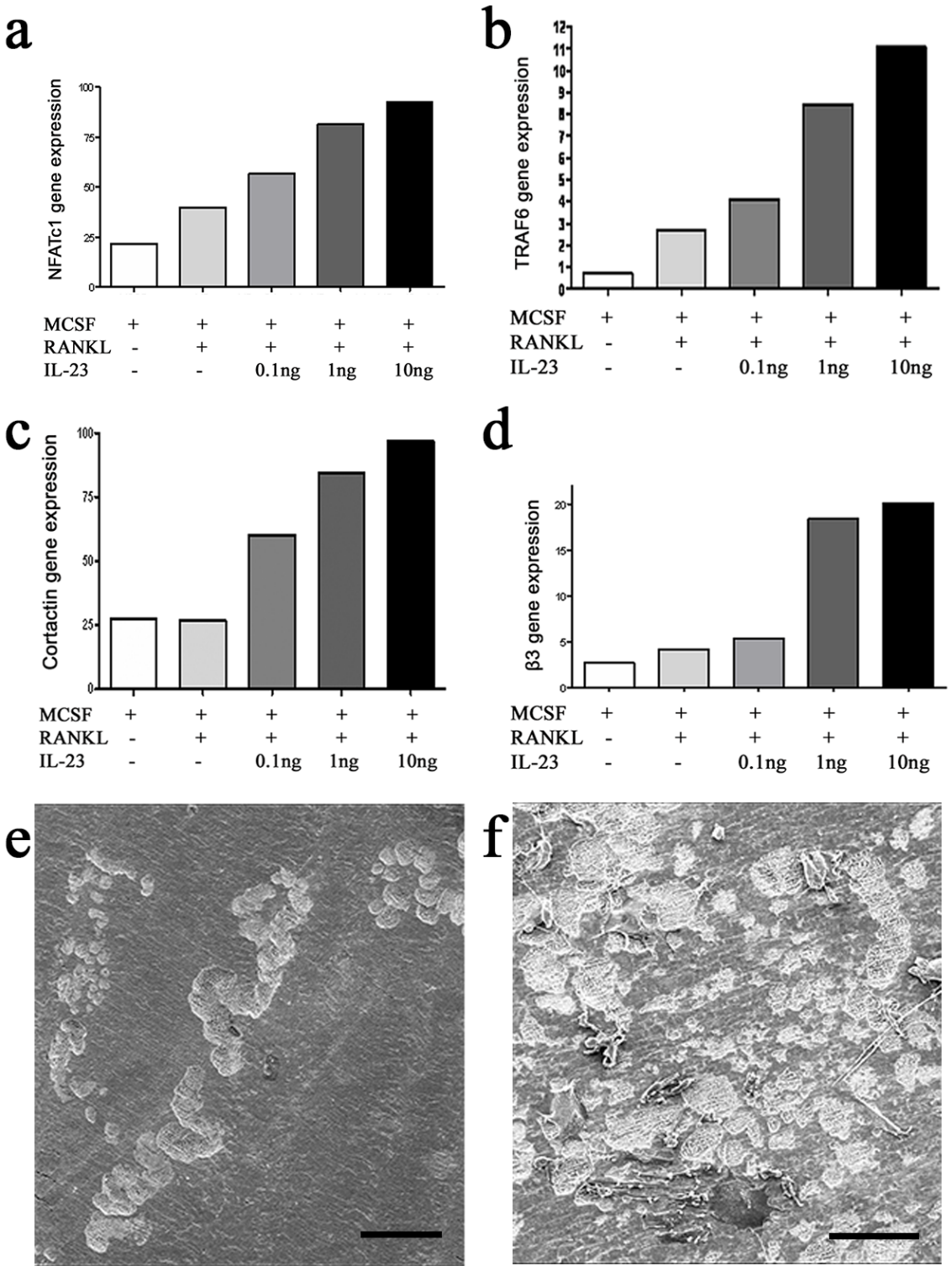

Supplementary Figure 2. IL-23 synergizes with RANKL to induce the expression of osteoclast-associated genes and bone resorption. Representative IL-23 induced gene expression of PBMC treated with increasing doses of IL-23 (0.1, 1, 10 or 100 ng/ml) in the presence of MCSF (25ng/ml) and RANKL (30ng/ml) showing the dose dependent increase in the osteoclast associated genes **a)** NFATC1, **b)** *TRAF6,* **c)** *CTTN* and **d)** *ITGB3*. Dose response data from one healthy donor. Representative scanning electron microscopy photomicrographs of PBMC cultured on dentine slices for 18 days in the presence of **e)** MCSF + RANKL or **f)** MCSF + RANKL + IL-23 (Bars represent 70 and 120 μm respectively).